Conference on Modelling Fluid Flow (CMFF'25)
The 19th International Conference on Fluid Flow Technologies
Budapest, Hungary, August 26-August 29, 2025

Impact of Wave Directionality and Inter-Device Spacing on the Performance of Wave Energy Converter Arrays

Anulekha Majumdar[1], Govindarajulu Venkatesan[2], Abdus Samad[3]

[1] Corresponding Author. Ocean Engineering Department, IIT Madras, Chennai, India, Energy and Fresh Water Department, National Institute of Ocean Technology, Chennai, India. E-mail: anulekha.niot@gmail.com
[2] Energy and Fresh Water Department, National Institute of Ocean Technology, Chennai, India. E-mail: gvenkat@niot.res.in
[3] Ocean Engineering Department, IIT Madras, Chennai, India. E-mail: samad@iitm.ac.in

ABSTRACT

It is well known that there is no significant effect on the wave power extraction from individual devices beyond a certain spacing between the wave energy converters (WEC) in an array, as destructive interference is reduced. However, this arrangement would require a huge amount of money, which would have cost implications. Moreover, restrictions in the available area might limit this arrangement. Hence, exploring alternate wave spacing arrangements is required to optimize the layout. There is no effect of wave directionality on the power obtained for a single-point absorber wave energy device. However, when considering a wave farm, the WEC layout will be affected by the direction of incoming waves. Studies have shown that for the Indian coast, the maximum wave power is observed during the monsoon period, from waves originating from wave direction between 245 - 270 °, which are South westerlies. Thus, it is imperative to consider the wave direction as an important parameter. The paper aims to study the effect of wave directionality, WEC spacing, and layout on wave power. A two-body point absorber is considered for the study.

Keywords: hydrodynamic analysis, point absorbers, time domain simulation, wave energy converter farms, wave farm layout

NOMENCLATURE

F_e	$[N]$	excitation force
F_{ext}	$[N]$	external force
F_{hs}	$[N]$	hydrostatic restoring force
F_r	$[N]$	radiation force
F_v	$[N]$	viscous drag force
g	$[m/s^2]$	Earth's acceleration
m	$[kg]$	mass matrix
m_a	$[kg]$	added mass matrix
ω	$[rad/s]$	wave frequency
ϕ	$[m^2/s]$	velocity potential function
ϕ_D	$[m^2/s]$	diffraction wave potential
ϕ_I	$[m^2/s]$	incident wave potential
ϕ_R	$[m^2/s]$	radiation wave potential
τ	$[s]$	past time
ζ	$[m]$	motion amplitude
A_∞	$[kg]$	instantaneous added mass effect
d	$[m]$	water depth
j	[]	degree of freedom
$K(t-\tau)$	$[kg/s]$	Impulse response function
n	$[m^2/s]$	unit normal vector of the body surface pointing outwards
t	$[s]$	present time
x	$[m]$	position vector
Z	$[m]$	vertical coordinate of a wetted surface

Abbreviations

BEM	Boundary element method
BEMIO	Boundary element method Input/Output
IRF	Impulse response function
JONSWAP	Joint North Sea Wave Project
LA	Line absorber
PA	Point absorber
PTO	Power take-off
WEC	Wave energy converter

1. INTRODUCTION

Wave energy is a renewable energy source that is available in abundance from the oceans. It has a very high energy density; however, the waves are highly dynamic in nature. For the coastal areas near the equator, the waves have lower heights, resulting in lower extractable power. India is such a place. However, it has a vast coastline, with many places having higher wave activity. In addition, many coastal areas lack adequate power and drinking water facilities. Hence, the coastal areas can be supplied with power by utilising a wave energy converter (WEC),

which converts the motion of the waves into electricity in a sustainable way. An optimised array of WEC can extract power from waves on a MW scale. This power can then be used for many things, such as generating potable water from the oceans. Several studies have carried out life cycle analyses for conventional fossil fuel electricity plants and a wave energy farm and reported a 20-40 times reduction in the carbon footprint. To reach the stage of commercialization, WECs need to be grouped in a particular arrangement, considering the wave conditions, the hydrodynamic interactions of the devices, and the cost of the technology. Using models and machine learning techniques, a single wave energy device has previously been optimized for its shape, control method, and power take-off (PTO) system.

1.1. Literature review

Budal conducted the first study on wave arrays [1]. He introduced the concept of point absorber theory and coined the term interaction factor or q factor, which is defined as the power produced by the array to the sum of the power produced by the devices when present individually. q>1 signifies constructive interference, and q<1 represents destructive interference. Thereafter, Falnes [2] and Evans [3] carried out studies on point absorber (PA) arrays to obtain a *q factor* of more than 1. McIver [4] in 1994 studied the change of the q factor with changing wave direction. He also studied the effect of equal and unequal spacing between WECs. Fitzgerald and Thomas [5], in 2007, conducted a study on five WECs considering the effect of the geometry of the WEC and the direction of the wave.

India has a wave energy potential of 40 GW [6], with the southern tip having the highest potential. Researchers studied various WECs for various locations along the Indian coast, for offshore and nearshore conditions [7, 8], and observed that multibody PA and line absorbers (LA) performed better for nearshore and offshore locations, respectively. However, in these studies, a single WEC was considered, with no effect of the directional characteristics or the hydrodynamic changes owing to other devices in the array. In addition, the significant wave height considered was less than 1.5 m, when the maximum significant wave height occurring in the Indian coastal waters can go up to 3 m. Waves of maximum height were also observed to come from 245 - 270 ° [9]. So, it is imperative to understand the effect on power produced due to changing wave direction and the presence of multiple WECs.

Cruz et al. [10] analysed a single-body PA farm with 4 WECs arranged in a square layout for regular and irregular waves. Regular waves are sinusoidal waves with the same wave height and period. Irregular waves can be defined as the superposition of many regular waves of different wave heights and periods. By changing the incident wave angle and applying suboptimal control of the external damping coefficient, they observed a 4% increase in power when the direction was changed from 90 to 45 °. De Andres et al. [11] studied a farm layout of 2-body WEC for optimizing the q factor by analysing wave layout, spacing, the number of WECs, and wave direction. Increasing the number of WECs increased the q factor. The highest q factor was obtained for half of the wavelength of the incident wave; triangle or rhombus layouts were good for multidirectional waves, and square for unidirectional waves; q factor results were similar for triangle and square layouts. Ji et al. [12] studied a circular layout for a six two-body PA array and concluded that as the radius of the circle increased, power first increased, then decreased, and eventually stabilized. They also studied the effect of change in wave direction on power and found power to vary negligibly. However, for a farm of 2 WECs, there was a change in power with changing wave directions. Murai et al. [13] studied array arrangement, incident wave angle, optimal control parameters to maximize power generation, and linear and triangular configurations and drew similar conclusions for linear arrays as de Andres et al. [11]. They also observed that PTO damping had a larger influence on power change than PTO stiffness; also, poor arrangement can negate the effect of choosing optimal control parameters.

This paper presents the study of WEC arrays to understand the effect of wave direction on it. Here, two layouts are studied—3 and 5 devices. Time domain simulations are carried out to estimate the power for both regular and irregular waves. The effect of device spacing is also investigated.

2. WEC MODEL

WEC performance evaluation is carried out in two steps. First is frequency domain calculation, where the problem is linearised, allowing for simplification using linear potential flow theory. The governing equations are transformed into the frequency domain, leading to a set of algebraic equations. This approach assumes harmonic excitation, making it computationally efficient. The Boundary Element Method (BEM) is the most commonly adopted numerical technique for solving this problem. BEM determines the excitation forces, radiation damping, and added mass coefficients. The most popular software for this purpose are ANSYS AQWA, WAMIT, and NEMOH. Since the WEC considered here is a point absorber, that is, the diameter of the device is much smaller than the wavelength of the wave, and the wave conditions are relatively mild, this problem can be solved using potential flow theory. The hydrodynamic coefficients were determined in the linear potential flow BEM solver AQWA. In AQWA, the panel method is used to compute the device's hydrodynamic coefficients. The software considers the following assumptions:

- Bodies have negligible forward speed

- Fluid is inviscid and incompressible
- Flow is irrotational
- Incident wave amplitude are small compared to the wavelength

Assuming a velocity potential function for the body $\phi(x,t)$, the body should satisfy the Laplace equation as follows

$$\nabla^2\phi = 0 \tag{1}$$

The solution of the Laplace equation is based on the boundary conditions considered and the decomposition of the solution into diffraction and radiation forces.
Boundary condition 1: Linear free surface equation

$$-\omega^2\phi + g\frac{\partial\phi}{\partial Z} = 0 \quad on \quad Z = 0 \tag{2}$$

where ω is the wave frequency, g is the Earth's acceleration, and Z is the vertical coordinate of the wetted surface.
Boundary condition 2: Body surface conditions:

$$\frac{\partial\phi}{\partial n} = \begin{cases} i\omega n_j & for \quad radiation \quad potential \\ -\frac{\partial\phi}{\partial n} & for \quad diffraction \quad potential \end{cases} \tag{3}$$

on the mean wetted surface of the body.
where n is the unit normal vector of the WEC surface pointing outwards.
Boundary condition 3: Seabed surface condition at water depth d

$$\frac{\partial\phi}{\partial Z} = 0 \quad on \quad Z = -d \tag{4}$$

A far field radiation boundary condition needs to be considered for the wave to dissipate at a distance.

$$\sqrt{(x^2+y^2)} \to \infty \tag{5}$$

ϕ can be decomposed into

$$\phi = \phi_I + \phi_D + \phi_R \tag{6}$$

where ϕ_I is the incident wave potential, which is the wave potential in the absence of the WEC, ϕ_D is the diffracted wave potential, which is the wave potential due to interaction between the incident wave and a motionless WEC, and ϕ_R is the radiated wave potential, which is the wave field produced by the WEC motion in the absence of any wave. The radiation potential can be expressed as

$$\phi_R = i\omega\sum_{j=1}^{6}\zeta_j\phi_j \tag{7}$$

where ζ_j is the motion amplitude in the jth mode and ϕ_j is radiated potential from body motion in the jth mode. From the radiation potential, added mass and frequency damping are obtained by evaluating the hydrodynamic forces induced by unit motions in each degree of freedom. The excitation force in each degree of freedom is computed from the incident and diffracted wave potentials.
The output from the BEM software is fed into a time domain-based solver. BEMIO (Boundary Element Method Input/Output), an open-source Python library used for hydrodynamic analysis of floating bodies, interfaces with BEM solvers to extract and process hydrodynamic coefficients. It converts hydrodynamic coefficients from the frequency domain to the time domain by computing impulse response functions (IRFs) using the Cummins equation framework. It creates an .h5 file, which, along with the Simulink model and WEC geometry, is given as an input to WEC-Sim, an open-source tool developed in MATLAB, to obtain the power output of the WECs, which is the second step to evaluate the WEC performance. WEC-Sim solves the Cummins equation. The time domain equation of motion for the WEC, with its origin at the centre of gravity, can be represented by Eq. 8 as

$$(m+m_a)\ddot{x} = -F_r + F_e - F_{hs} + F_v + F_{ext} \tag{8}$$

where, m = mass matrix, m_a = added mass matrix at infinite frequency, x = position vector, F_r= radiation force, F_e= excitation force vector, F_{hs} = hydrostatic restoring force vector, F_v = viscous drag force vector, and F_{ext}= external force vector. In the present study, only the heave motion is considered. Therefore, all quantities reduce to scalars. The radiation and excitation forces together constitute the hydrodynamic force. The hydrodynamic simulation models determine the dynamic response of a system or group of devices based on the forces in the above equation. The Cummins equation describes the motion of the WEC due to waves, taking into account the interaction between fluid and structure. The radiation force can be split into two parts: the instantaneous added mass effect, $A_\infty\ddot{x}(t)$ and the convolution integral, $\int_0^t K(t-\tau)\dot{x}(\tau)d\tau$. Therefore, F_r can be represented as

$$F_r = A_\infty\ddot{x}(t) + \int_0^t K(t-\tau)\dot{x}(\tau)d\tau \tag{9}$$

where $K(t-\tau)$ is the IRF, which tells how the force depends on the previous velocities of the WEC, at a time lag $(t-\tau)$, t is the current time at which the forces have to be evaluated, and τ is the past time, ranging from the start of the simulation to the present time, $\dot{x}(\tau)$ describes the past velocities at time τ. These frequency-domain coefficients are converted into the time domain by calculating the IRF. Thus, the Cummins equation takes the following form:

$$(m+m_a)\ddot{x} + A_\infty\ddot{x}(t) + \int_0^t K(t-\tau)\dot{x}(\tau)d\tau = F_e - F_{hs} + F_v + F_{ext} \tag{10}$$

The left-hand side of the equation includes inertia, memory (via convolution), and restoring forces. The right-hand side includes excitation force, viscous damping, and external forces. WEC-Sim uses these

IRFs to solve the Cummins equation and compute motion and power. The system is represented using mathematical blocks in Simulink. The bodies are defined as rigid bodies, which are connected to each other using constraint blocks or a PTO block. A linear spring damper PTO was considered for the study. Figure 1 shows a flowchart illustrating the sequence of steps involved in calculating the power output of the WEC. A study was undertaken to select the appropriate WEC for the farm by considering a single and a two-body WEC [14]. It was observed that the two-body WEC produced 28% higher power than the single-body WEC, thus being the device considered for further studies. Fig. 2 shows the WEC considered for study, and Table 1 shows the dimensions of the WEC. Two configurations of wave farms were studied: a 3-device and a 5-device farm. Several researchers observed that a triangular layout gave better results compared to other layouts, such as linear and square layouts [15, 11]. Hence, for the 3-device and 5-device configurations, a triangular layout was considered, as shown in Figures 3 and 4. A pentagon layout was not considered for analysis previously. Hence, a pentagon layout was considered for the 5-device configuration, as shown in Fig. 5. A 2 m wave height and 6 seconds period were considered.

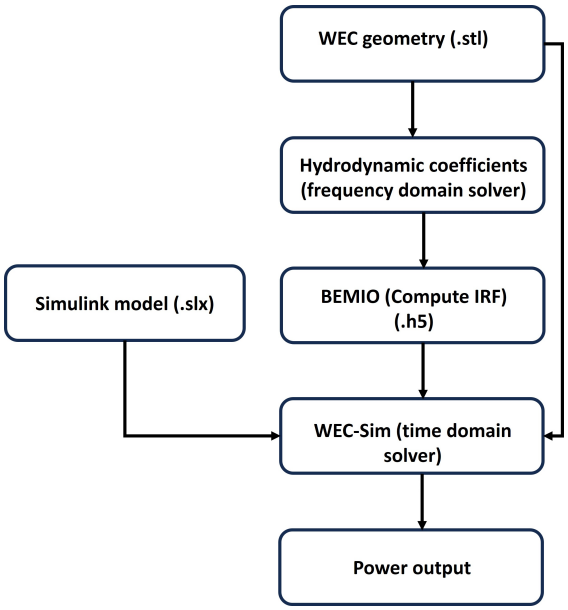

Figure 1. Steps for Calculating WEC Power Output

Table 1. Dimensions of the two-body WEC

Parameter	Value
Diameter of buoy	3 m
Height of buoy	0.8 m
Draft	0.25 m
Diameter of sphere	3.9 m

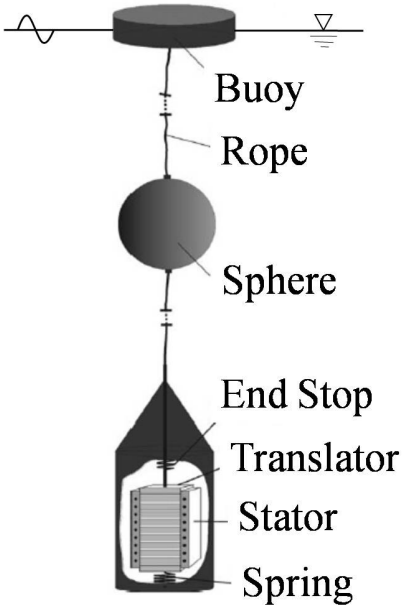

Figure 2. Two-body PA [16]

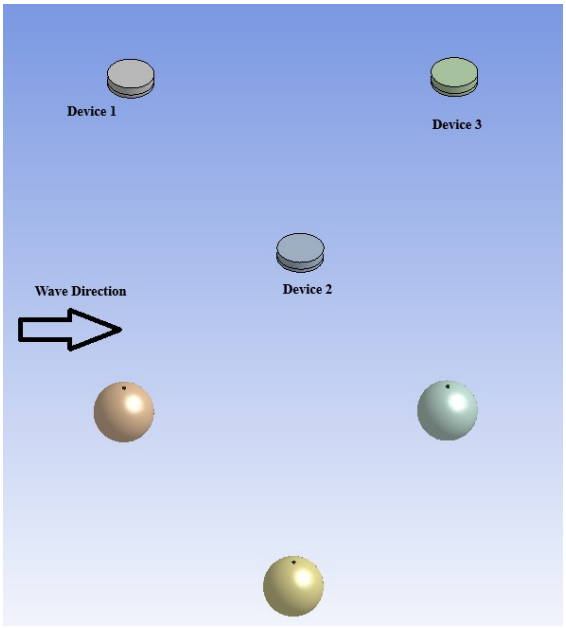

Figure 3. 3-device configuration

3. NUMERICAL RESULTS

3.1. Effect of layout

First, the number of devices on the farm was studied for regular and irregular waves. Irregular waves can be described using many spectra. Here, a Joint North Sea Wave Project or JONSWAP spectrum was used [17]. The inter-device spacing was fixed at 20 m. Figures 6, 7, and 8 show the power obtained for a 3-device and 5-device configuration in regular wave conditions. Here, the 0° incident wave direction was considered. Negative power val-

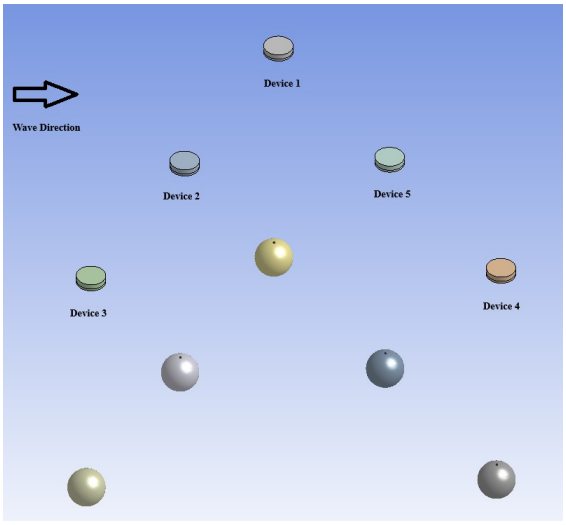

Figure 4. 5-device configuration in triangular layout

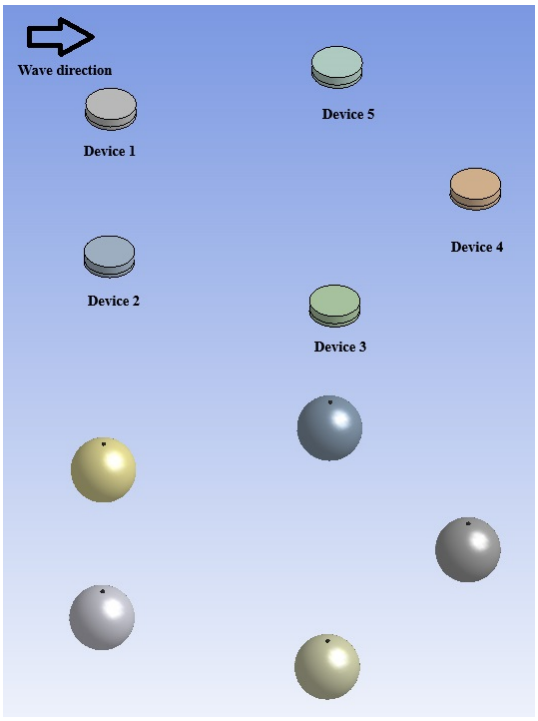

Figure 5. 5-device configuration in pentagon layout

ues indicate energy absorption from waves, as per the WEC-Sim sign convention. It was observed that the power obtained for a 3-device configuration for an individual device is more than the 5-device configuration. Figures 9, 10, and 11 show the average power obtained for a 3-device and 5-device configuration in irregular wave conditions. Even for irregular waves, the power obtained for individual devices in the triangular configuration is more than that of the pentagon configuration.

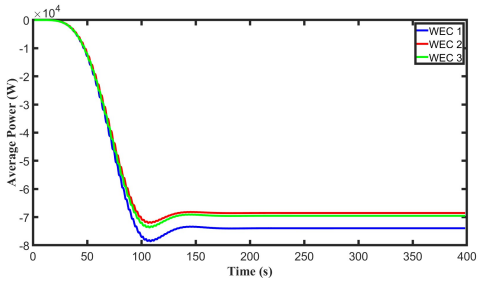

Figure 6. Power obtained for a three-device configuration in regular waves

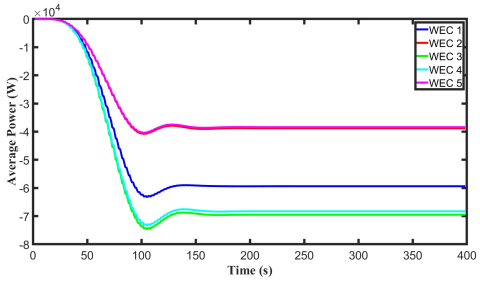

Figure 7. Power obtained for a five-device triangular configuration in regular waves

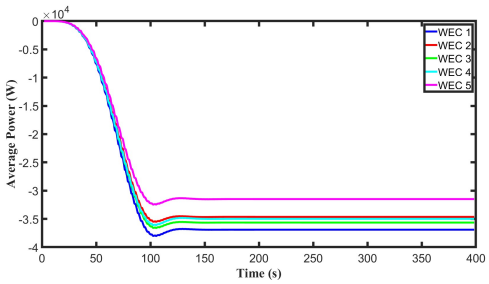

Figure 8. Power obtained for a five-device pentagon configuration in regular waves

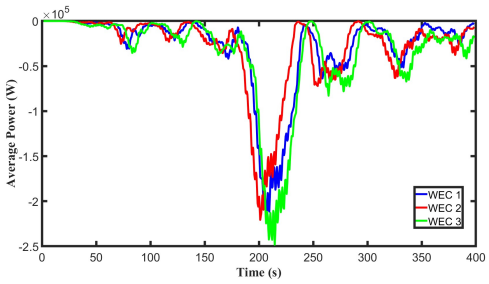

Figure 9. Power obtained for a three-device configuration in irregular waves

3.2. Effect of wave direction

To understand the effect of wave direction, the 5-device triangular layout with 20 m spacing was studied. Fig. 12 shows the comparison of average power for the triangular layout for 8 wave directions: 0, 30,

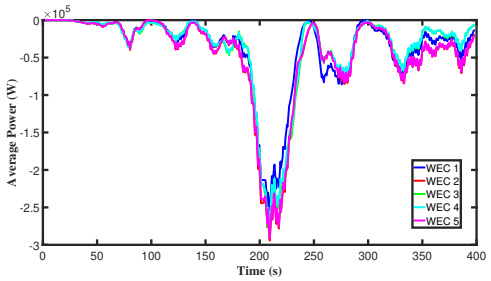

Figure 10. Power obtained for a five-device triangular configuration in irregular waves

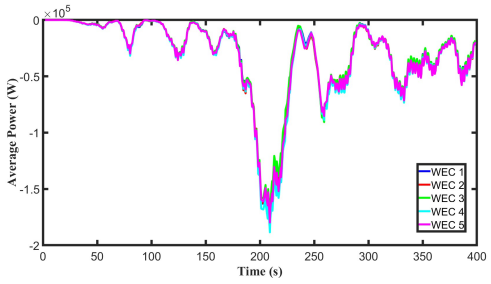

Figure 11. Power obtained for a five-device pentagon configuration in irregular waves

45, 60, 90, 135, 180, and 270 °. The maximum average power was obtained for an incident wave direction of 0 °, followed by 180 °, 30 °, then 45 °, 135 °, 60 °, 270 ° and lastly 90 °.

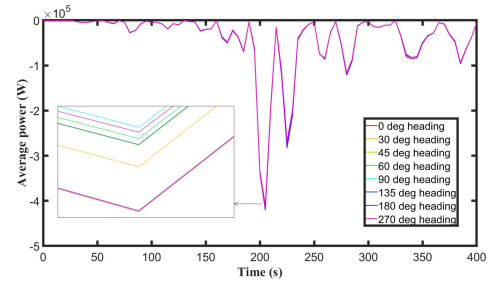

Figure 12. Power obtained for different wave directions for five-device triangular layout configuration

3.3. Effect of device spacing

Three device spacings were studied for the triangular configuration of 3 devices: 10 m, 20 m, and 30 m for regular wave conditions. From Figures 6, 13 and 14, it can be observed that the devices in the farm with 10 and 20 m spacing have varying power, with the device encountering the wave first having maximum power and subsequent devices having lesser power, whereas the farm with 30 m spacing all have the same power. Babarit [18] observed that for smaller arrays of smaller-diameter buoys, the separating distance should be 10 to 20 times the diameter to avoid any interference between the motion of the neighboring devices. If the spacing is less than this, the power produced from these interacting devices will be reduced.

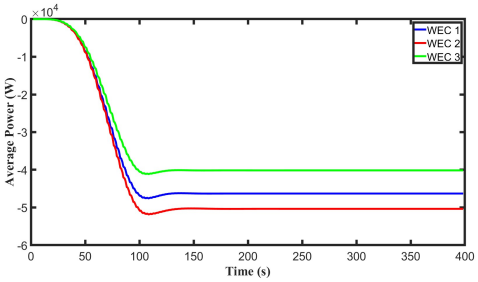

Figure 13. Power obtained for the farm of 10 m spacing for three-device triangular layout

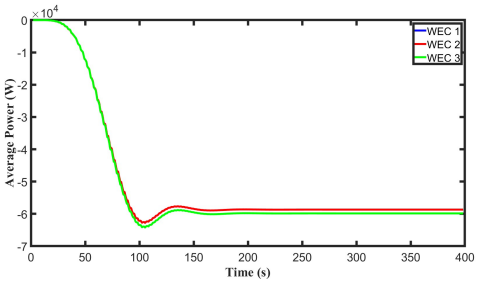

Figure 14. Power obtained for the farm of 30 m spacing for three-device triangular layout

4. CONCLUSION

The paper discusses the effect of layout, wave direction, and spacing between devices on the power produced by the wave farm. After obtaining the hydrodynamic coefficients in Ansys AQWA, the power produced was calculated using the time-domain simulation tool WEC-Sim. Only the heave direction was considered for power calculation. A 3- and 5-device farm was studied for both regular and irregular waves, where it was found that for the triangular layout, the power produced by the individual device was almost twice that of the individual device of the pentagon layout for both wave conditions. Also, for the triangular layout, the power produced by the individual devices in the 5-device configuration was more than the 3-device configuration. Consequently, the effect of incident wave direction was studied, and it was found that maximum power was obtained for a wave at 0 °. Lastly, varying the spacing between the devices, it was observed that a device spacing of the order of 10 times the diameter eliminated any destructive interference, whereas, for lesser device spacing of the order of 3 to 4 times the diameter of the device, the movement of one device affected that of the subsequent devices, reducing the power produced by them.

REFERENCES

[1] Budal, K., 1977, "Theory for absorption of wave power by a system of interacting bodies", *Journal of Ship Research*, Vol. 21 (04), pp. 248–254.

[2] Falnes, J., 1980, "Radiation impedance matrix and optimum power absorption for interacting oscillators in surface waves", *Applied Ocean Research*, Vol. 2 (2), pp. 75–80.

[3] Evans, D., 1981, "Maximum wave-power absorption under motion constraints", *Applied Ocean Research*, Vol. 3 (4), pp. 200–203.

[4] McIver, P., 1994, "Some hydrodynamic aspects of arrays of wave-energy devices", *Applied Ocean Research*, Vol. 16 (2), pp. 61–69.

[5] Fitzgerald, C., and Thomas, G., 2007, "A preliminary study on the optimal formation of an array of wave power devices", *Proceedings of the 7th European Wave and Tidal Energy Conference, Porto, Portugal*, pp. 11–14.

[6] Sannasiraj, S., and Sundar, V., 2016, "Assessment of wave energy potential and its harvesting approach along the Indian coast", *Renewable Energy*, Vol. 99, pp. 398–409.

[7] Patel, R. P., Nagababu, G., Kachhwaha, S. S., Surisetty, V. A. K., and Seemanth, M., 2023, "Techno-economic analysis of wave energy resource for India", *Journal of the Indian Society of Remote Sensing*, Vol. 51 (2), pp. 371–381.

[8] Amrutha, M., and Kumar, V. S., 2022, "Evaluation of a few wave energy converters for the Indian shelf seas based on available wave power", *Ocean Engineering*, Vol. 244, p. 110360.

[9] Amrutha, M. M., and Sanil Kumar, V., 2016, "Spatial and temporal variations of wave energy in the nearshore waters of the central west coast of India", *Annales Geophysicae*, Vol. 34 (12), pp. 1197–1208.

[10] Cruz, J., Sykes, R., Siddorn, P., and Taylor, R. E., 2009, "Wave farm design: preliminary studies on the influences of wave climate, array layout and farm control", *Proceedings of the 8th European Wave and Tidal Energy Conference, Uppsala, Sweden*.

[11] De Andrés, A., Guanche, R., Meneses, L., Vidal, C., and Losada, I., 2014, "Factors that influence array layout on wave energy farms", *Ocean Engineering*, Vol. 82, pp. 32–41.

[12] Ji, R., Sheng, Q., Wang, S., Zhang, Y., Zhang, X., and Zhang, L., 2019, "Array characteristics of oscillating-buoy two-floating-body wave-energy converter", *Journal of Marine Science and Application*, Vol. 18, pp. 325–333.

[13] Murai, M., Li, Q., and Funada, J., 2021, "Study on power generation of single Point Absorber Wave Energy Converters (PA-WECs) and arrays of PA-WECs", *Renewable Energy*, Vol. 164, pp. 1121–1132.

[14] Majumdar, A., Venkatesan, G., and Samad, A., 2024, "Numerical Analysis and Validation of Point Absorber Wave Energy Converters for the Indian Coast", *ISOPE Pacific/Asia Offshore Mechanics Symposium*, ISOPE, pp. ISOPE–P.

[15] Borgarino, B., Babarit, A., and Ferrant, P., 2012, "An implementation of the fast multipole algorithm for wave interaction problems on sparse arrays of floating bodies", *Journal of Engineering Mathematics*, Vol. 77, pp. 51–68.

[16] Engström, J., Eriksson, M., Isberg, J., and Leijon, M., 2009, "Wave energy converter with enhanced amplitude response at frequencies coinciding with Swedish west coast sea states by use of a supplementary submerged body", *Journal of Applied Physics*, Vol. 106 (6).

[17] Kumar, V. S., and Kumar, K. A., 2008, "Spectral characteristics of high shallow water waves", *Ocean Engineering*, Vol. 35 (8-9), pp. 900–911.

[18] Babarit, A., 2013, "On the park effect in arrays of oscillating wave energy converters", *Renewable Energy*, Vol. 58, pp. 68–78.